UCRL-JC-125626
PREPRINT

Deformation and Velocity Measurements at Elevated Temperature in a Fractured 0.5 M Block of Tuff

S.C. Blair
P.A. Berge

This paper was prepared for submittal to the
NY Rocks 97 Conference, 36th U.S. Rock Mechanics Symposium
New York, NY
June 29-July 2, 1997

February 1996

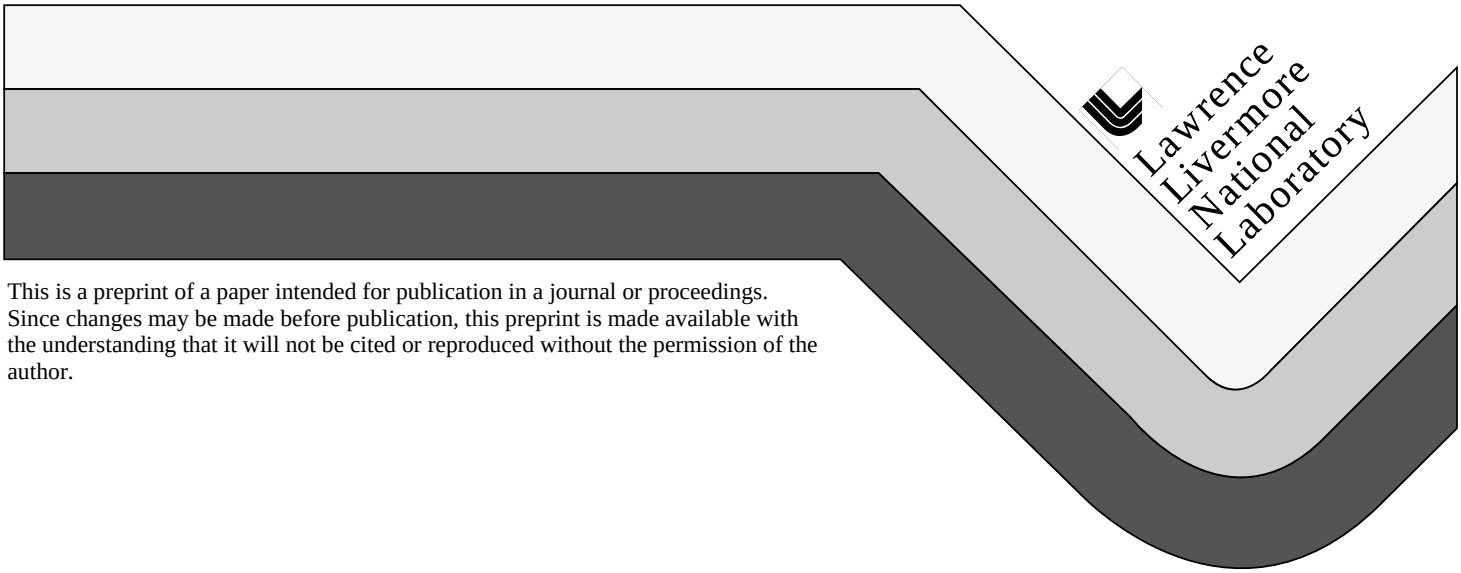

Int. J. Rock Mech. & Min. Sci. Vol. 34, No. 3-4, 1997
ISSN 0148-9062

To cite this paper:
Int. J. Rock Mech. & Min. Sci. **34:3-4,** Paper No. 030

DEFORMATION AND VELOCITY MEASUREMENTS AT ELEVATED TEMPERATURE IN A FRACTURED 0.5 M BLOCK OF TUFF

S. C. Blair and P. A. Berge

Lawrence Livermore National Laboratory
PO Box 808, L-201, Livermore, CA 94551 USA
(Internet: blair5@llnl.gov, berge1@llnl.gov)

ABSTRACT

This paper presents preliminary results of laboratory tests conducted on small block samples of Topopah Spring tuff, in support of the Yucca Mountain Site Characterization Project. The overall objective of these tests is to investigate the thermal-mechanical, thermal-hydrological, and thermal-chemical response of the rock to conditions similar to the near-field environment (NFE) of a potential nuclear waste repository. We present preliminary results of deformation and elastic wave velocity measurements on a 0.5-m-scale block of Topopah Spring tuff tested in uniaxial compression to 8.5 MPa and at temperatures to 85˚C. The Young's modulus was found to be about 7 to 31 GPa for vertical measurements (parallel to the stress direction) across parts of the block containing no fractures or a few fractures, and 0.5 to 0.9 GPa for measurements across individual fractures, at ambient temperature and 8.5 MPa maximum stress. During stress cycles between 5 and 8.5 MPa, the deformation modulus values for the matrix with fractures were near 15-20 GPa at ambient temperature but dropped to about 10 GPa at 85˚C. Compressional wave velocities were found to be about 3.6 to 4.7 km/s at ambient temperature and stress. After the stress was cycled, velocities dropped to values as low as 2.6 km/s in the south end of the block where vertical cracks developed. Heating the block to about 85˚C raised velocities to as much as 5.6 km/s in the upper third of the block.

KEYWORDS

Fractures, Young's Modulus, Temperature Effects, Mechanical Properties, Radioactive Waste, Rock Properties, Scale Effects, Laboratory Tests, Compressional Wave Velocity

INTRODUCTION

This paper presents preliminary results of laboratory testing of a small block sample of Topopah Spring Tuff. This is the first in a series of tests on small block samples, conducted in support of the Yucca Mountain Site Characterization Project. The purpose of these tests is to investigate the thermal-mechanical, thermal-hydrological, and thermal-chemical response of the rock to conditions similar to the near-field environment (NFE) of a potential nuclear waste repository. This paper presents preliminary results of deformation and

elastic wave velocity measurements on a 0.5-m-scale block of Topopah Spring tuff tested in uniaxial compression and at temperatures to 85˚C.

Data at this scale are needed to provide input to models used for analysis of the repository, as data from smaller samples commonly tested in the laboratory do not provide information on fracture behavior, and very few data sets are available from in situ rock masses. Moreover, tests at this scale have the benefit that known boundary and environmental conditions (such as uniaxial stress and a uniform temperature field) can be imposed on a rock sample that contains multiple fractures, while field data are often poorly constrained due to inherent limitations on boundary conditions, instrumentation coverage, and material characterization. These tests are the first of a series of tests designed to study coupled processes in the near-field environment of a nuclear waste repository. Deformation and elastic wave velocity data provide an approximation of total rock mass (i.e., matrix plus fractures) mechanical properties and behavior for welded tuff units that contain fractures and vugs, and guidance for input values used in equivalent continuum models of a repository. These results provide constraints on how the flow and transport properties of the rock in the very near-field region of a repository may change as the temperature and stress fields change over time. This paper describes the test methodology, presents deformation and compressional wave velocity measurements for a small block tested at elevated temperature and pressure, and discusses results.

APPARATUS AND METHODOLOGY

Block Sample Description

Blocks of Topopah Spring tuff were excavated from the Large Block Test (Lin et al., 1995) site on Fran Ridge at Yucca Mountain, Nevada, and were then cut into rectangular prisms having dimensions of several tens of cm. Photos of the rock and digitized maps of the fractures in the blocks are presented in Blair and Berge (1997). A review of Topopah Spring tuff properties can be found in Wilder (1996). The block used in the tests described in this paper has dimensions of 64 cm $\times$ 32 cm $\times$ 25 cm. The sample exhibits the typical Topopah Spring tuff fabric of subparallel vugs in pink and gray densely welded tuff. It contains several high-aspect-ratio vugs oriented roughly parallel to the foliation. The block was cut so that the vugs and foliation are subparallel to the longest dimension.

Loading Frame and Vertical Stress Measurement

The apparatus used for testing small blocks in compression is a 300-ton loading frame that can accommodate samples up to 1 m $\times$ 1 m in cross section and 2 m in height, thus allowing testing of samples up to 2 m^3 in volume. The vertical load is applied via 12 hydraulic actuators that are mounted in the cross-head and operated in tandem. The large sample size afforded by this apparatus allows testing of samples that contain multiple fractures and heterogeneities such as vugs. For all tests conducted in this study, the press was operated in uniaxial compression only, to a maximum stress of ~8.5 MPa. The pressure in the actuators that supplied the vertical load was monitored manually from a pressure gauge and recorded using a computerized data acquisition system described in Blair and Berge (1997). The vertical stress on the sample was computed using the pressure supplied to the loading actuators, the cross section of the pistons in the actuators, and the horizontal cross section of the sample. For the tests discussed in this paper, the sample was loaded into the frame so that the shortest dimension was parallel to the applied vertical stress, as shown in Figure 1.

Displacement Measurements

Deformation was measured using linear displacement transducers (direct-current displacement transducers or DCDTs). Initially nine displacement transducers were used (some are shown on west side of block in Figure 1), but more were added after the first sequence of testing. The final locations of the transducers on the four sides of the block are illustrated in Figure 2. Some of the transducers monitored displacement over the entire height of the block while others measured the deformation of individual fractures or zones of unfractured

rock matrix. Displacement measured by a DCDT was determined from voltages, and strain over the measured length for a given DCDT was then calculated from the displacement so that stress-strain curves could be plotted and Young's modulus values could be found from the slopes of the curves.

Heaters and Temperature Measurements

Part of the testing described in this paper was conducted at elevated temperatures. For the high-temperature tests, the sample was heated from the top and bottom using two heater/insulation stacks, including the following components: a 3.2-mm layer of Teflon, heaters, and a 1.6-mm-thick copper plate cut to size for the top and bottom surfaces of the sample. Two 15-watt foil heating elements were attached to each copper plate along with a thermocouple to measure the temperature near each heating element. The heaters are discussed in more detail in Blair and Berge (1997). This configuration was found to produce nearly uniform temperatures across the block face. The heater plate was separated from the rock surface using the 3.2-mm Teflon sheet. A 10-cm layer of a calcium silicate insulating material was placed between the heater plates and the loading platens at the top and bottom of the block. Household roll-type insulation (R30) was wrapped around the entire assembly to insulate the sides of the block. The heaters were powered using a manually-adjustable power supply. The heating elements were wired in parallel, and an input voltage between 0 and 34 volts was sufficient to heat the block. Temperature was measured at selected points located along a vertical line near the center of the sample and along a horizontal line in the midplane of the sample, using 12 thermocouples in the block.

Velocity Measurements

Heavily damped, 100-kHz transducers were used to measure compressional wave velocities in many locations for horizontal wave propagation through the tuff sample. For each measurement, the source and receiver transducers were positioned on opposite faces of the block (north and south faces or east and west faces), in alignment to measure horizontal propagation along the shortest direct path through the block (64 cm for north-south propagation and 32 cm for east-west paths). Velocities were not measured in the vertical direction because the block was sitting in the load frame and there was no access to the top or bottom of the block. Velocity anisotropy for the sample is expected to be less significant than velocity differences due to heterogeneity (Blair and Berge, 1997). Horizontal velocity measurements were made for all accessible parts of the block, with individual measurements made approximately every 5 cm along the block where the block's surface was accessible and up to 15 cm apart in places where the dense concentration of thermocouples or DCDTs made the block's surface inaccessible. The resulting measurements represent the horizontal velocities in the block adequately since a spacing of about 5 to 15 cm is equivalent to about one or two wavelengths for the typical measurement frequencies of about 50 to 200 kHz. Initial measurements were made at ambient pressure and temperature conditions, and velocity measurements were repeated at elevated stress and temperature conditions. Frequency dependence was not investigated because of cost considerations. Velocities were computed using the known distance across the block and the observed arrival time determined from the onset of the compressional wave identified in the time series. Most measurements had signal-to-noise ratios between 2:1 and 4:1 and timing uncertainties of about ± 2 μs, resulting in velocity uncertainties of approximately ± 0.1 km/s. Blair and Berge (1997) describe the velocity measurement system, calibrations, and results in detail. Here the velocity results are presented briefly together with the more detailed presentation of deformation results.

RESULTS

Description of the Load Path

Several loading/unloading cycles were imposed on the block. Initially, a loading sequence (Sequence #1) was imposed that consisted of a series of four loading/unloading cycles (#1a, #1b, #1c, #1d) in which the

maximum compressive stress, σ_1, was increased by approximately 2 MPa in each successive cycle, until a maximum compressive stress of approximately 8 MPa was applied. Displacement parallel to the applied stress was monitored at nine locations on the vertical surfaces of the block (some are shown on west side of block in Figure 1), with some of the transducers mounted across discrete horizontal fractures and/or vugs, and others monitoring displacement in unfractured regions as well as over the entire height of the block. Upon review of the data from Sequence #1, six additional displacement transducers were added to the block, and five additional loading/unloading cycles were completed (Sequence #2a-#2e), where σ_1 was increased by approximately 1.5 to 2 MPa in each successive cycle, up to a maximum stress of about 8.5 MPa in the last cycle. Compressional wave traveltimes were measured at ambient pressure after Sequence #2. The purpose of the cyclic, incremental loading was to (a) evaluate the testing apparatus, as it had not been used in this configuration before, and (b) evaluate hysteresis in the mechanical deformation from cycle to cycle.

A third sequence (Sequence #3) of loading/unloading cycles was performed that included cycling stress at temperatures of about 50 and 85˚C. Prior to this sequence, 12 thermocouples were mounted in the sample, and 6 of the displacement transducers were reconfigured to monitor horizontal deformation (see Figure 2). During Sequence #3 the sample was held at constant stress while temperature was slowly changed and/or compressional wave traveltimes were measured. The stress and temperature history of Sequence #3 is listed in Table 1.

TABLE 1
SUMMARY OF SEQUENCE #3 ACTIVITIES

Elapsed time (hr)	Activity
1	Cycle σ_1: 0.1 – 3.5 – 0.1 MPa
22	Increase σ_1 to 3.5 MPa, V_p at 3.5 MPa
90	Cycle σ_1: 3.5 – 8.5 – 5 MPa, V_p at 8.5 MPa
98	Cycle σ_1: 5 – 8.5 – 5 MPa, V_p at 8.5 MPa
250	Increase temperature to 50˚C
330	V_p at 5 MPa, 50˚C
495	Cycle σ_1: 5 – 4 – 7 – 5 MPa, V_p at 5 MPa, 50˚C
1200	Increase temperature to 80˚C, V_p at 5 MPa
1450	Increase temperature to 85˚C, σ_1= 5 MPa
1500	Cycle σ_1: 5 – 8.5 – 5 MPa
1530	Cool to 20˚C
1804	Cycle σ_1: 5 – 8.5 – 0.1 MPa

V_p indicates compressional-wave velocity measurement.

Rock Mass Deformation at Ambient Temperature

Testing at ambient temperature included all of Sequence #1 and #2 and the first 250 hours of Sequence #3. Results for Sequence #1 and #2 showed nonlinear, repeatable deformation with applied stress. Stress–strain curves representing deformation in Sequence #2d and #2e for a vertical DCDT spanning the entire block (matrix plus fractures) are shown in Figure 3. This figure shows that deformation is nonlinear with increasing stress, and that modulus increases as vertical stress increases above 4 MPa. The modulus value computed for vertical stress below 4 MPa is ~3 GPa, and that value increases to ~6 GPa as applied stress is raised above 4 MPa. These values are considerably lower than modulus values measured on core samples (e.g., Blair et al., 1996), and reflect the fact that the block contains vugs and fractures. The increase in

deformation modulus with increasing vertical stress can be attributed to closure of fractures and vugs that occur in a subhorizontal zone near the lower central portion of the block (see Blair and Berge, 1997). Moreover, the curve exhibits the banana shape that is associated with the hysteretic behavior of fractures. The hysteresis shown during the initial stage of unloading is attributed to the cohesion of fractures, where the stress drops from about 8.5 MPa to about 7.5 MPa without any change in strain. The plot shows that the cohesion for this zone is ~1 MPa, which is an order of magnitude weaker than values often used in numerical models of rock behavior that incorporate discrete joints and fractures. As the load continues to decrease, the slope of the unloading curve decreases gradually. The strain returns to the origin at the end of the unloading for each of the two cycles shown in Figure 3, and the loading curve for Sequence #2e coincides with the loading curve for #2d. This indicates that there was no significant amount of irreversible strain during this test. The results of this test provide guidance for parameter values assigned to the representative element volume (rev) used in equivalent continuum models, and are especially appropriate for analysis of the Topopah Spring tuff at Yucca Mountain because the size of the block (0.5-m-scale) is approximately the size of blocks forming the *in situ* rock mass (e.g., Wilder, 1996).

A typical stress–strain curve obtained for a vertical displacement transducer monitoring the matrix (area with no fractures or vugs) during Sequence #2e is shown in Figure 4 along with the Sequence #2e curve from Figure 3 showing strain over the total height of the sample. The stress–strain response for the matrix is nearly elastic (linear) over the range of applied stress. The deformation modulus computed from these data is approximately 7 GPa for the matrix, and approximately 3 to 6 GPa for the whole rock. Modulus measurements during Sequence #2 for matrix areas produced values as high as 31 GPa (see Blair and Berge, 1997), with all of the matrix regions showing linear elastic behavior. These values are consistent with, but somewhat lower than, those measured in laboratory tests on core samples (e.g., Blair et al., 1996).

The stress–strain response during Sequence #2e for a vertical DCDT crossing one of the horizontal fractures is shown in Figure 5. (Note that the strains are about an order of magnitude larger than values plotted in Figures 3 and 4.) The deformation data for single fractures is useful for evaluating inputs to discrete element models and some effective continuum models that incorporate the behavior of individual fractures. This fracture is perpendicular to the applied stress. Comparing the curve in Figure 5 to those in Figure 4, we see that the shape of the stress–strain curve for the single fracture shares a key characteristic of the curve for the total rock (matrix plus fractures). The curve in Figure 5 shows nonlinear behavior with a change in the slope of the curve when the applied stress is increased above approximately 2.5 to 4 MPa. Similarly, the curve in Figure 4 for the entire rock (matrix plus fractures) shows a distinct change in slope when the applied stress is increased above about 4 MPa. In contrast, the other curve in Figure 4 shows linear behavior for the matrix material instead of having a banana-shape. The curve in Figure 5 shows that the modulus for the fracture increases as vertical stress increases above 2.5 MPa from a value of about 0.5 GPa to about 0.9 GPa; this increase is attributed to fracture closure. The stress–strain curve in Figure 5 again indicates a cohesion value of about 1 MPa, since the strain did not change significantly when the stress was reduced from 8.5 MPa to about 7.5 MPa. Note that the stress–strain curve does not return to zero strain, indicating that some non-recoverable deformation did occur. This observation indicates permanent deformation of the fractures. One of the assumptions often made in analysis of fractured rock is that the mechanical response can be decomposed into components due to the matrix material and the fractures, respectively. The data collected during this experiment allow that assumption to be tested. Plots of displacement as a function of time (not shown) during Sequence #2e for transducers monitoring horizontal fractures and vuggy zones and for near-by transducers spanning the entire height of the block indicate that approximately 95% of the displacement measured by transducers crossing the entire block occurs across the fractures (see Blair and Berge, 1997). Thus we find that at this 0.5-m scale, in a rock with vugs and fractures, vuggy zones behave similar to horizontal fractures, the decomposition of displacement into matrix and fracture components is valid, and most of the displacement at stress levels up to 8.5 MPa occurs in the fractures.

The stress–strain behavior observed during Sequence #3 at stresses less than 4 MPa (1 and 22 hr) matched closely with that for Sequence #2. However, when stress was raised above 4 MPa, some of the measured deformation for Sequence #3 diverged significantly from that observed for Sequence #2 (see Blair and Berge, 1997). It is important to note that, as shown in Table 1, loading of the sample in Sequence #3 was done over a long period. A small amount of deformation at constant stress was observed during this period,

and this increased deformation at stresses above 4.0 MPa can be attributed to the closing of horizontal cracks and vugs in the sample. We also found that horizontal displacement along one surface (the west side) increased dramatically at stresses above 5 MPa. Vertical fractures in the region spanned by a horizontal displacement transducer were observed to have opened and apparently caused the expansion. (We did not have enough transducers to determine if horizontal displacement was high for all sides of the block, but it is likely that any differences found would indicate heterogeneity in the rock rather than uneven loading.) In addition, the stress cycles imposed at t = 90 and t = 98 in Sequence #3 yield values for the deformation modulus between 15 and 20 GPa, which are somewhat higher than values observed for Sequences #1 and #2. Additional stress-strain curves and plots of displacement vs. time can be found in Blair and Berge (1997).

Measured velocities in the block at ambient temperature and pressure just before Sequence #3 were found to be between about 3.6 and 4.7 km/s, in agreement with laboratory tests on cores (e.g., Martin et al., 1994). The velocities dropped when the stress was raised, having values of 3.1 to 4.5 km/s at about 4 MPa and 2.6 to 4.0 km/s at about 8.5 MPa applied stress. The drop in horizontal velocities is probably related to opening of vertical cracks and damage caused by repeated stress cycling. The velocity change after repeated stress cycling coincided with the increased horizontal displacement along the west side of the block, discussed above.

Finally, it is important to note that during Sequences #2d and #2e, noticeable spalling occurred at several locations on the block. This was not observed during any of the cycles in Sequence #1 nor in Sequences #2(a–c) and indicates that subcritical crack growth occurs even at very low stresses in this rock when it is subject to cyclic loading. This may be relevant for evaluating the effect of seismic shaking of the potential repository over long times and at elevated temperature and humidity, because the velocity of subcritical crack growth is known to increase as temperature and humidity are increased.

Testing at Elevated Temperature

The sample was also tested at elevated temperature as shown in Table 1. The vertical stress was cycled between approximately 5 and 8.5 MPa while the sample was held at temperatures of approximately 50 and 85˚C for a period of 2 months, and the stress was cycled again after the block was allowed to cool to room temperature. Temperatures were monitored continuously at 12 locations in the block. Detailed plots of the temperature distribution in the block at different times during the test can be found in Blair and Berge (1997).

Stress–strain data for the three temperatures are shown in Figure 6. This figure includes the stress–strain data for the ambient-temperature phase of loading Sequence #3. This figure shows the following features: (1) The stress-strain curves for 50 and 85˚C are offset to the right of the curve for 23˚C, indicating that deformation occurred at constant stress while the sample was heated to temperature and held at temperature. (2) The modulus decreases as temperature is increased. (3) The stress–strain curves at elevated temperature exhibit a stepwise behavior.

Detailed examination of data from the transducers measuring the complete height of the block indicates that the loading/unloading modulus decreased from about 19 GPa for the unheated case to 10 GPa for the rock at about 85˚C. This is a reduction of about a factor of two. Data for transducers that monitored matrix material similarly indicate that increasing the temperature reduced the matrix modulus by approximately a factor of two. One other observation is that at the higher temperatures, the matrix appears to contribute more to the deformation than it does at the lower temperatures.

The compressional wave velocities measured in the block were observed to increase with elevated temperatures. Observed velocities were about 2.8 to 4.5 km/s for temperatures near 50˚C, and about 3.2 to 5.6 km/s for temperatures near 85˚C. The increased velocities may indicate closure or healing of vertical cracks at elevated temperatures.

Stress–strain data for unloading from 8.5 MPa after the sample had cooled from 85 to 23˚C showed that significant deformation remained in the sample. (See Blair and Berge, 1997 for additional plots). The observed unloading modulus was 11 GPa, similar to that observed in the heated rock. A permanent strain of

~0.0034 determined from the stress-strain curve after cool-down and unloading was verified by comparing measurements of the block dimensions from before and after the test. Moreover, measurements on the block also show that it grew shorter, and broader with lateral expansion of the block. The lateral expansion is somewhat misleading, however, because a significant amount of near-surface slabbing occurred on the vertical faces during the test.

DISCUSSION AND CONCLUSIONS

In this study a 0.5-m-scale block of welded tuff was subjected to a series of 1-day loading tests, and to a long-term thermal–mechanical test in which elevated temperatures and stresses were imposed on the sample for a period of approximately 2 months. Preliminary analysis indicates cycling compressive stress in 1-day tests produced nonlinear but repeatable behavior in the 0.5-m-scale block, with most of the deformation occurring across cracks, vugs and fractures. Imposing low levels of compressive stress for periods of a few days caused time-dependent, non-repeatable behavior to occur for cracks oriented both parallel and perpendicular to the applied stress. Under the long-term loading, cracks/vugs oriented perpendicular to the applied stress showed significant closure beyond that observed in the 1-day tests. In addition, the long-term loading caused pre-existing hairline cracks oriented in the direction parallel to the applied stress to open, which significantly reduced compressional wave velocities. Increasing temperature caused closure of some of the vertical cracks, which increased the velocities. Increasing the temperature also caused a softening of the mechanical response in the direction of loading.

These results have significant implications for the flow and transport properties of the rock in the very near-field region of a repository, as they indicate that some important properties of the rock mass may become increasingly anisotropic with time. For instance, if cracks, vugs, and fractures oriented perpendicular to the maximum principal stress undergo time-dependent closing, permeability in this direction will be reduced and deformation modulus will increase. Moreover, opening of pre-existing hairline cracks that occur near the drift wall and are oriented parallel to it will increase the permeability in this direction, and will change the geochemical environment by exposing different mineral assemblages.

Most deformation in the block occurred in vuggy zones and along fractures. The scale dependence of the deformation modulus measured for tuff is related to the different contributions of fractures and the rock matrix. Deformation measured in cores would be representative of the rock matrix only, whereas we were able to make measurements across individual fractures, unfractured matrix material, and across regions of the block that are representative of combined fracture and rock matrix stiffnesses. We found that the matrix material is up to an order of magnitude stiffer than the fractured rock, and the fractured rock is an order of magnitude stiffer than an individual fracture.

Noticeable spalling occurred at several locations on the block, indicating that subcritical crack growth can occur even at very low stresses in this rock when it is subject to cyclic loading. This may be relevant for evaluating the effect of seismic events on the potential repository over long times. More experiments will provide additional data on the geomechanical behavior at elevated temperature and humidity.

Acknowledgments

S. Trettenero, O. Pine, S. Daveler, S. Wood, K. Keller, and J. Kelly provided technical support. This work was supported by the Yucca Mountain Site Characterization Project. Work performed under the auspices of the U.S. D.O.E by Lawrence Livermore National Laboratory under contract W-7405-ENG-48.

References

Blair, S. C., Kelly, J. M., Pine, O., Pletcher, R., and Berge, P. A. (1996), *Effect of Radiation on the Mechanical Properties of Topopah Spring Tuff*, UCRL-ID-122899, Lawrence Livermore National Laboratory, Livermore, CA.

Blair, S. C., and Berge, P. A. (1997), *Geomechanical Properties of Topopah Spring Tuff at the 0.5 m Scale: Preliminary Results of Compression Tests at Elevated Temperature*, UCRL-ID-125089, Lawrence Livermore National Laboratory, Livermore, CA.

Lin, W., Wilder, D., Blink, J., Berge, P., Blair, S., Brugman, V., Carlson, R., Lee, K., Owens, M., Pletcher, R., Rector, N., Roberts, J., Ruddle, D., Sommer, S., Ueng, T., and Wagoner, J. (1995). The Large Block Test, A Progress Report. *Proceedings of the Sixth Annual International Conference on High Level Radioactive Waste Management, Las Vegas, NV, April 30-May 5, 1995*, American Nuclear Society, La Grange Park, IL, 46-47.

Martin, R. J., Price, R. H., Boyd, P. J., and Noel, J. S. (1994), *Bulk and Mechanical Properties of the Paintbrush Tuff Recovered from Borehole USW NRG-6: Data Report*, SAND93-4020, Sandia National Laboratories, Albuquerque, NM.

Wilder, D. G. (1996), *Near-Field and Altered-Zone Environment Report, Volume II*, UCRL-LR-124998, Lawrence Livermore National Laboratory, Livermore, CA.

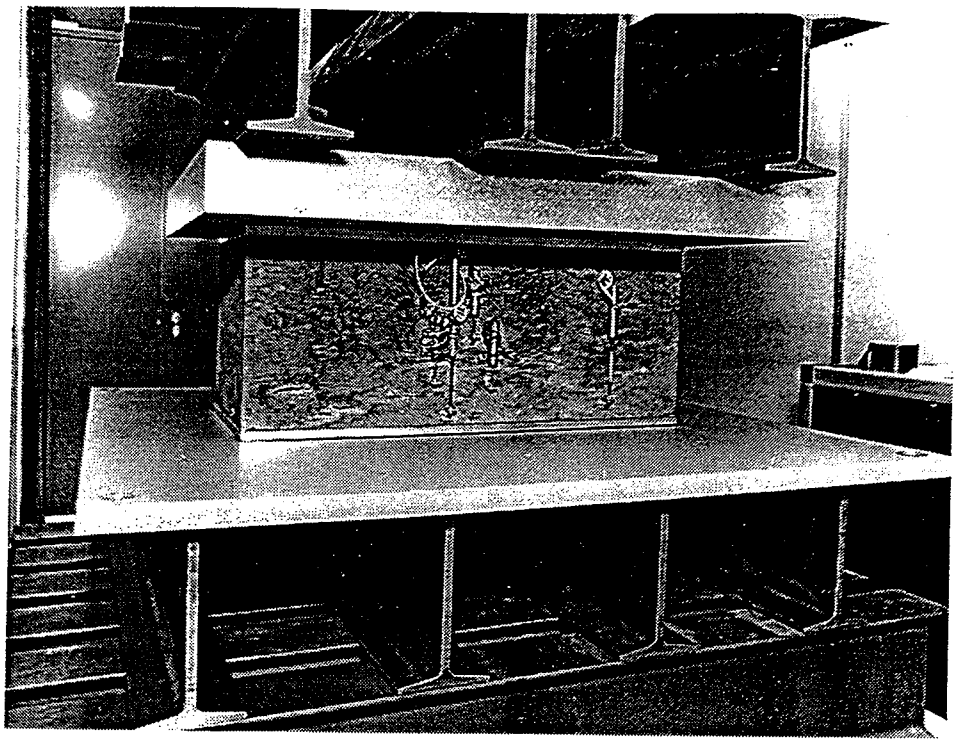

Figure 1: Small block sample (west side), assembled into load frame prior to test Sequence #1.

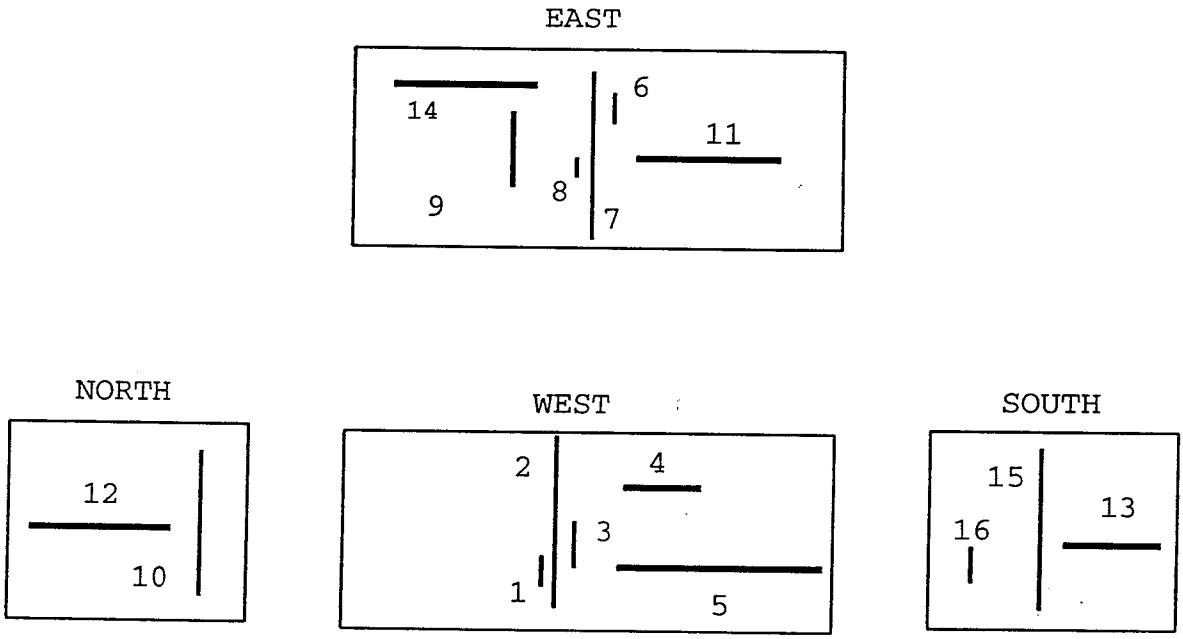

Figure 2: Displacement transducer locations on 4 faces of small block sample.

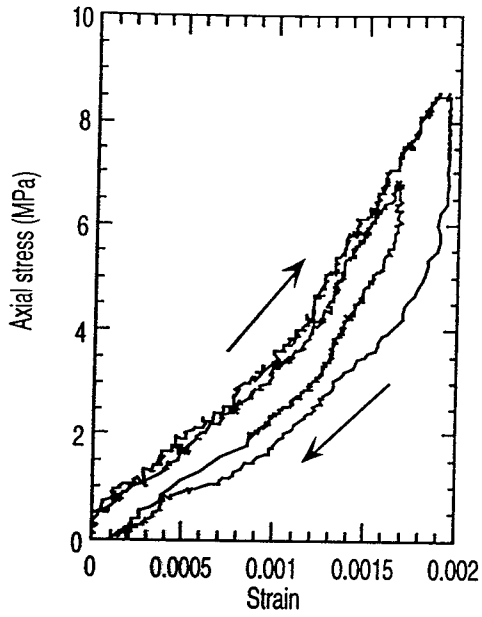

Figure 3: Stress-strain curve for measurements across total height of sample, for two stress cycles applied during Sequence #2.

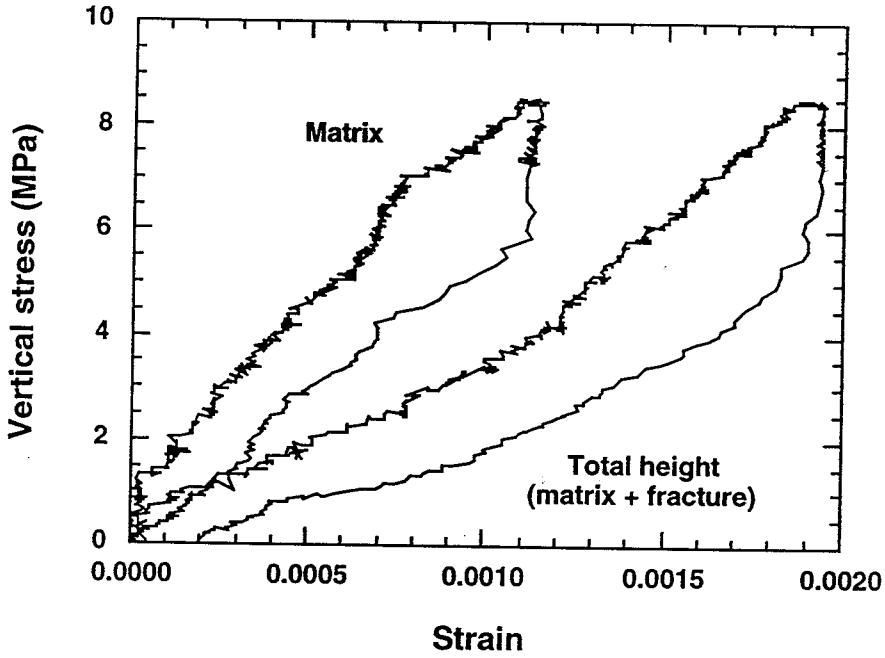

Figure 4: Stress-strain curves measured for matrix material and for the total height of the sample.

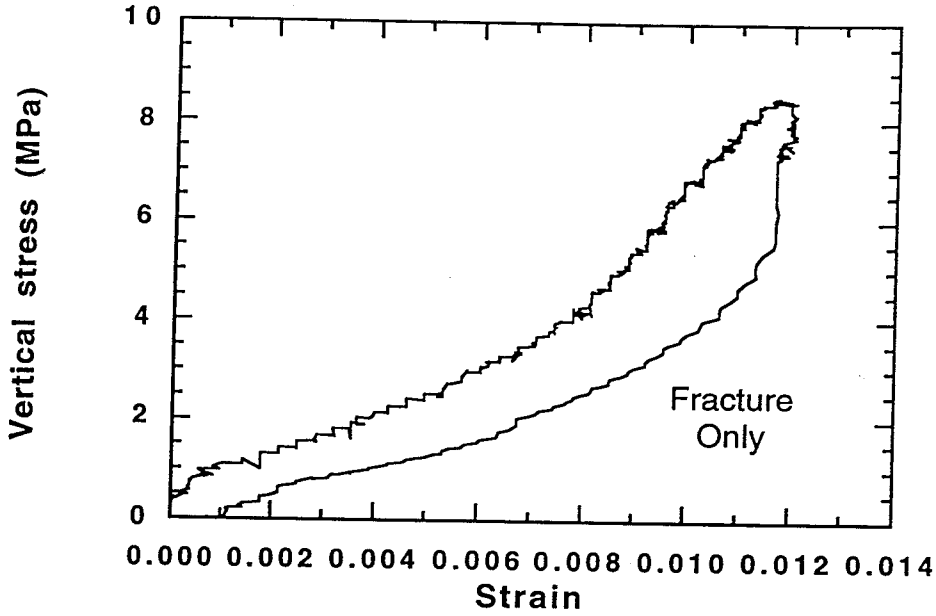

Figure 5: Stress-strain curve measured over a discrete fracture.

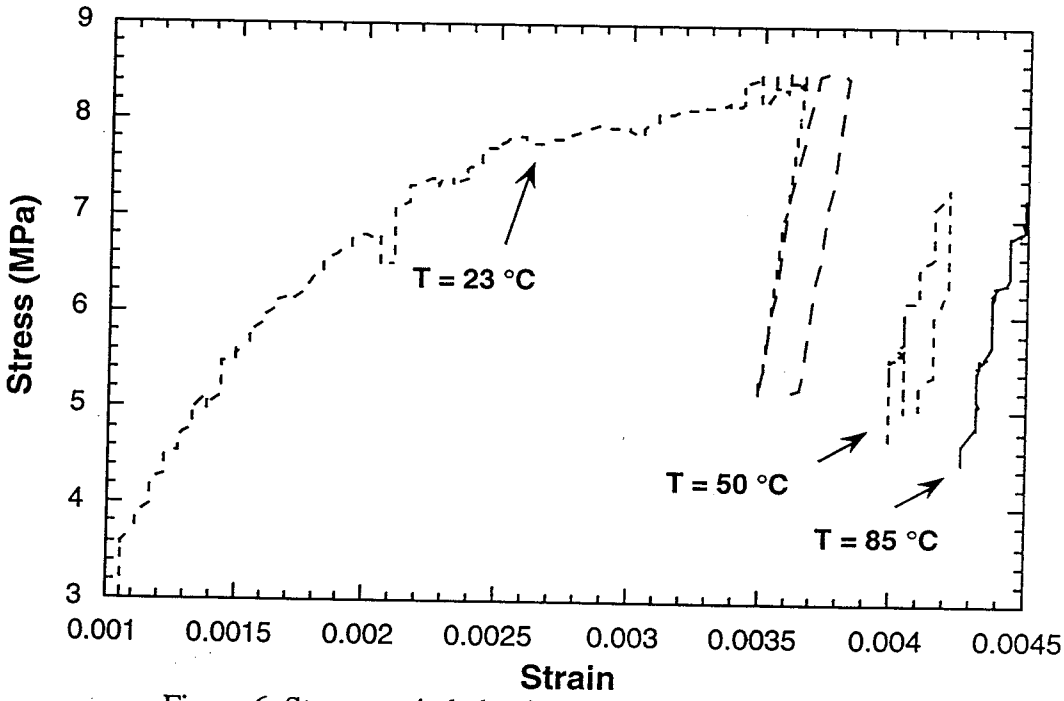

Figure 6: Stress-strain behavior at elevated temperature.

Technical Information Department • **Lawrence Livermore National Laboratory**
University of California • Livermore, California 94551